Atomically Precise Rhodium-Indium Carbonyl Nanoclusters: Synthesis, Characterization, Crystal Structure and Electron-Sponge Features.

Guido Bussoli,[a] Alberto Boccalini,[a] Marco Bortoluzzi,[b] Cristiana Cesari,[a] Maria Carmela Iapalucci,[a] Tiziana Funaioli,[c] Giorgia Scorzoni,[a] Stefano Zacchini,[a] Silvia Ruggieri,[*a,d] Cristina Femoni.[*a]

[a] Department of Industrial Chemistry "Toso Montanari", University of Bologna, Via Gobetti 85, 40129 Bologna, Italy

[b] Department of Molecular Sciences and Nanosystems, Ca' Foscari University of Venice, Via Torino 155, 30170 Mestre (VE), Italy

[c] Department of Chemistry and Industrial Chemistry, University of Pisa, Via Moruzzi 13, 56124 Pisa, Italy

[d] Laboratory of Luminescent Materials, Department of Biotechnology, University of Verona and INSTM, UdR Verona, Strada Le Grazie 15, 37134 Verona, Italy

*cristina.femoni@unibo.it; silvia.ruggieri@univr.it

SUPPORTING INFORMATION

LIST OF CONTENT

IR and ESI mass spectra for $[Rh_{12}In(CO)_{28}]^{3-}$ (1).

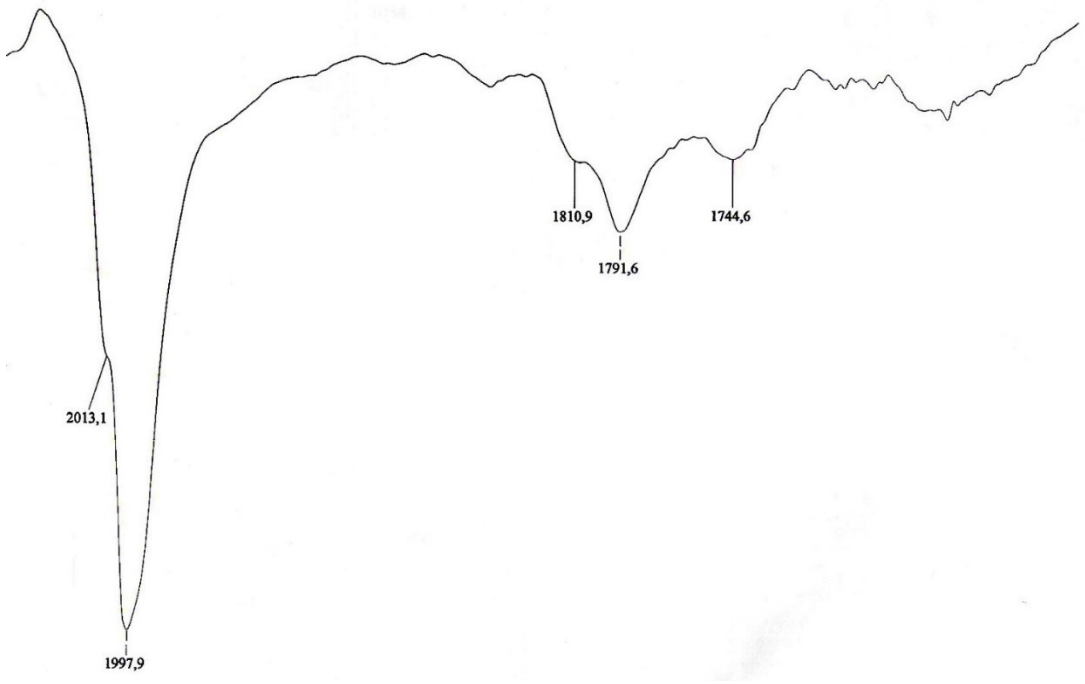

Figure S1a. IR spectrum of $[Rh_{12}In(CO)_{28}][NEt_4]_3$ registered in CH_3CN solution.

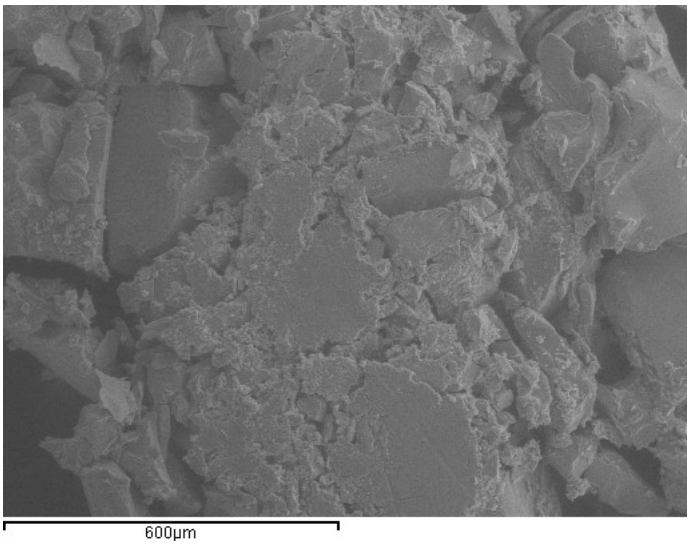

Figure S1b. SEM image of $[Rh_{12}In(CO)_{28}][NEt_4]_3$.

Element	% Spectrum 1	% Spectrum 2	% Spectrum 3	% Spectrum 4	Mean	Std Dev.
Rh	Atomic 93.56	Atomic 90.90	Atomic 90.95	Atomic 93.46	92.22	1.49
	Weight 92.87	Weight 89.95	Weight 90.01	Weight 92.76	91.40	1.64
In	Atomic 6.44	Atomic 9.10	Atomic 9.05	Atomic 6.54	7.78	1.49
	Weight 7.13	Weight 10.05	Weight 9.99	Weight 7.24	8.60	1.64

Table S1a. EDS analyses on different areas of a selected crystal of $[Rh_{12}In(CO)_{28}][NEt_4]_3$

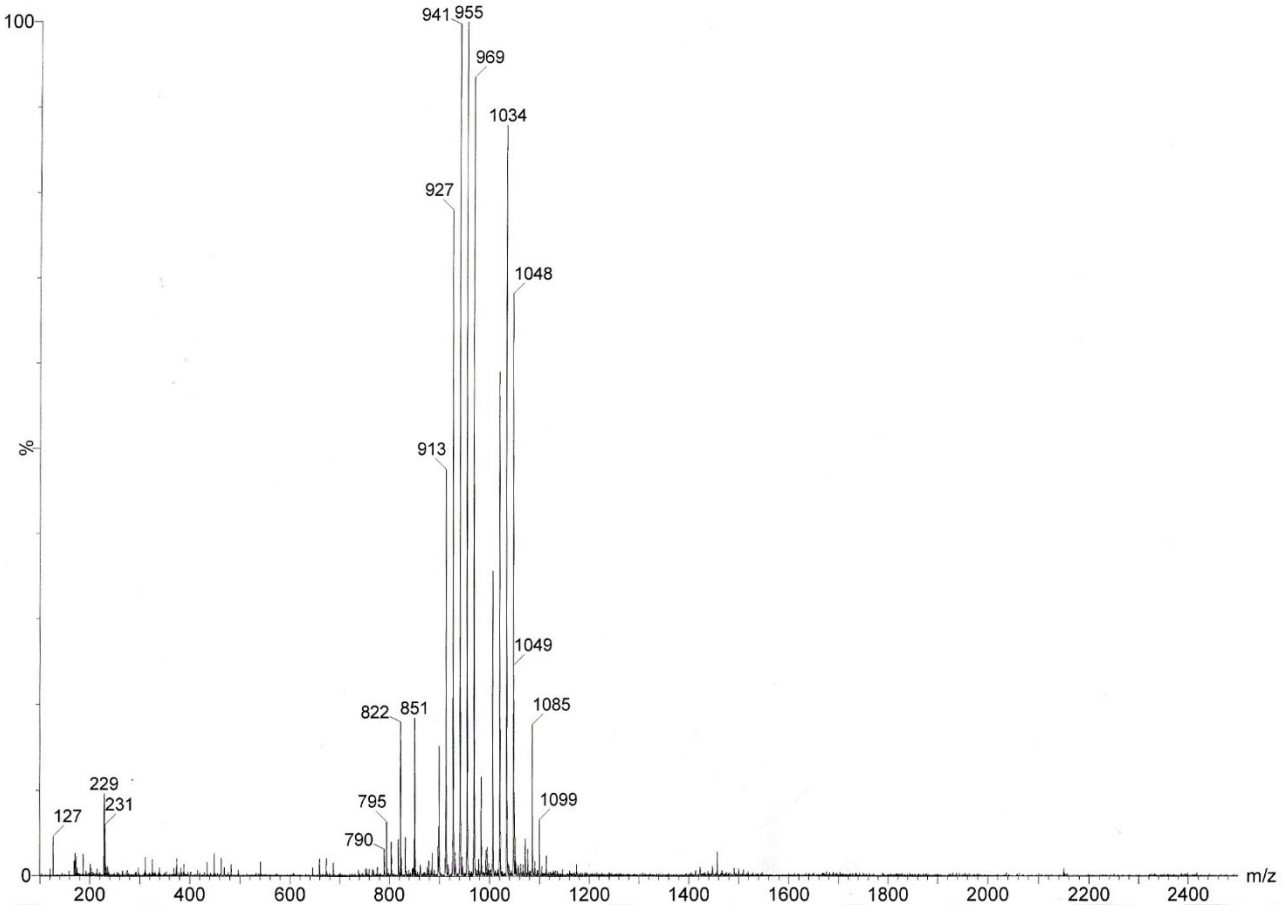

Figure S1c. ESI-MS of $[Rh_{12}In(CO)_{28}][NEt_4]_3$ registered in CH_3CN solution.

Most relevant signals (m/z)	Corresponding Ions
1113-1099-1085-1072	$\{[Rh_{12}In(CO)_{22\text{-}21\text{-}20\text{-}19}][NEt_4]_2\}^{2-}$
1048-1034-1020-1006	$\{[Rh_{12}In(CO)_{22\text{-}21\text{-}20\text{-}19}][NEt_4]\}^{2-}$
983-969-955-941-927-913-899	$[Rh_{12}In(CO)_{22\text{-}21\text{-}20\text{-}19\text{-}18\text{-}17\text{-}16}]^{2-}$
851-822-795	$[Rh_5(CO)_{12\text{-}11\text{-}10}]^{-}$

Table S1b. ESI-MS peak assignments for $[Rh_{12}In(CO)_{28}][NEt_4]_3$.

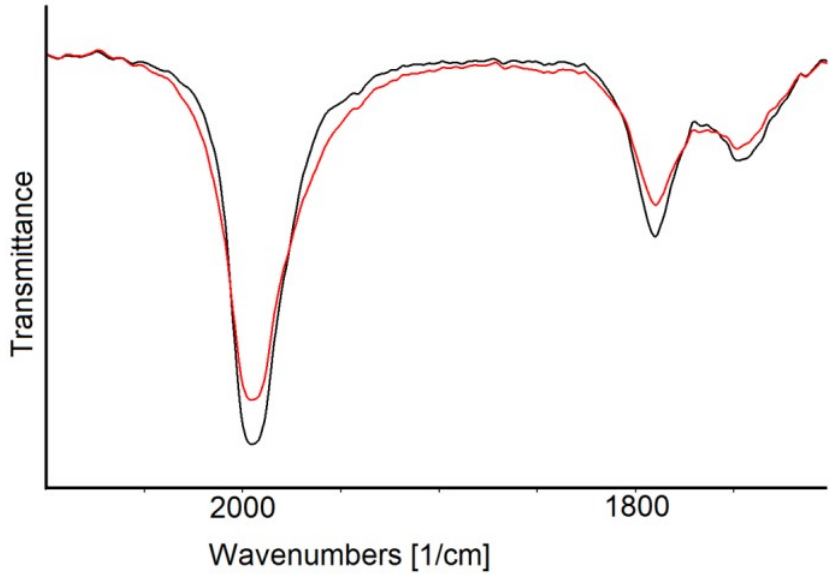

Figure S1d. IR spectra of a CH_3CN solution of $[Rh_{12}In(CO)_{28}]^{3-}$ recorded in an OTTLE cell before (black line) and after (red line) a cyclic voltammetry between –0.40 to +0.50 V *vs* Ag pseudo reference electrode (scan rate 1 mV sec^{-1}). $[N^nBu_4][PF_6]$ (0.1 mol dm^{-3}) as the supporting electrolyte. The solvent and supporting electrolyte absorptions have been subtracted.

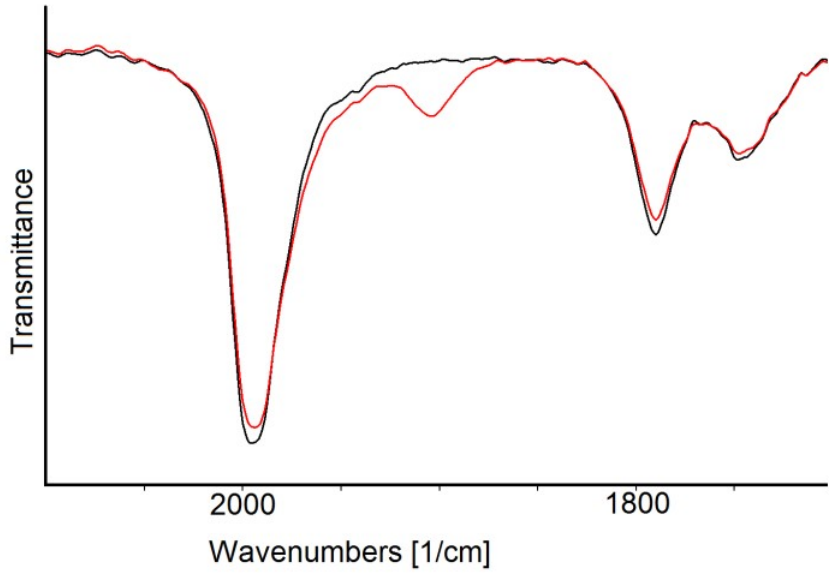

Figure S1e. IR spectra of a CH_3CN solution of $[Rh_{12}In(CO)_{28}]^{3-}$ recorded in an OTTLE cell before (black line) and after (red line) a cyclic voltammetry between to –0.40 and –1.85 V *vs* Ag pseudo reference electrode (scan rate 1 mV sec^{-1}). $[N^nBu_4][PF_6]$ (0.1 mol dm^{-3}) as the supporting electrolyte. The absorptions of the solvent and supporting electrolyte have been subtracted.

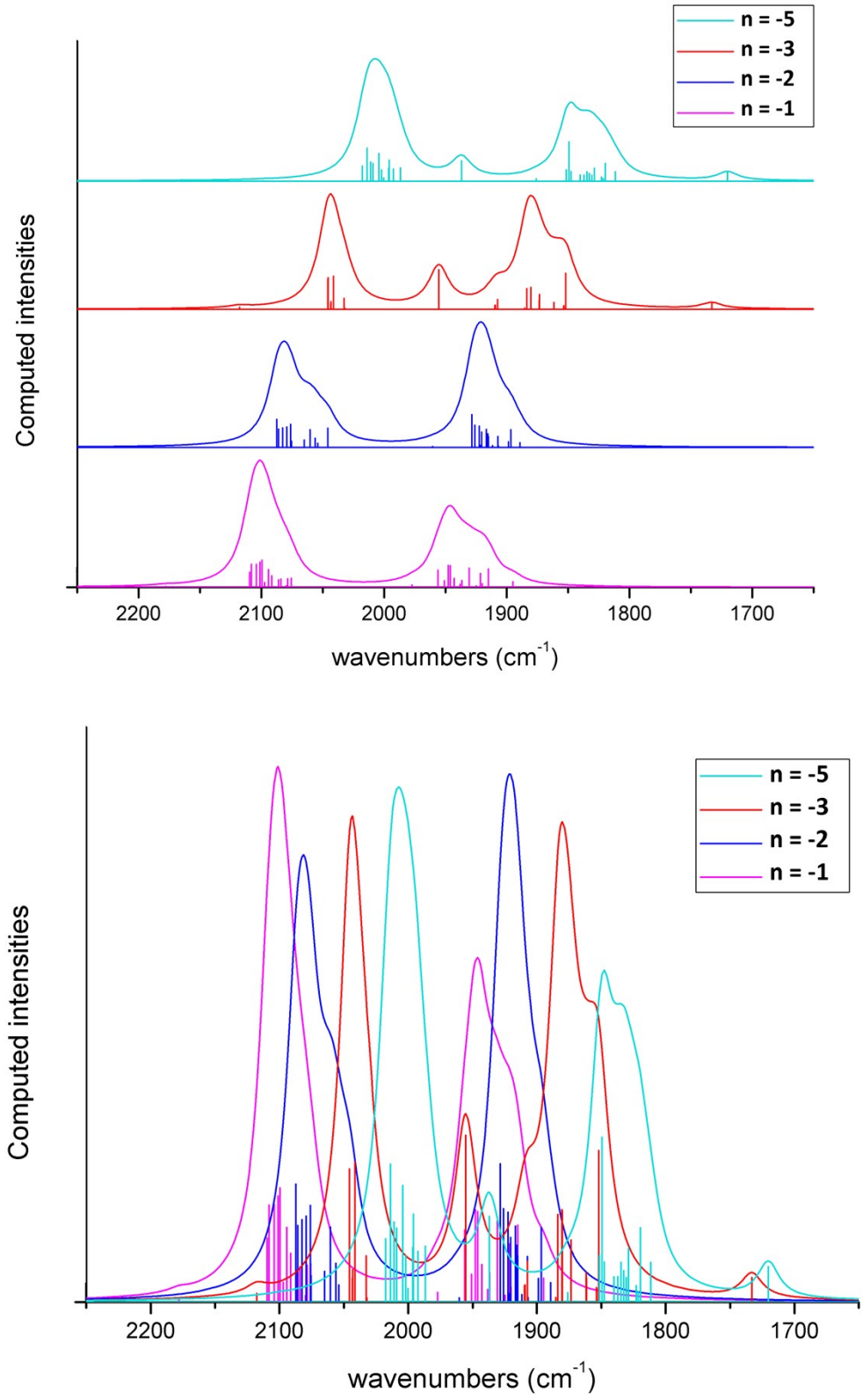

Figure S1f. Carbonyl regions of the simulated IR spectra (GBSA/GFN1-xTB) of $[Rh_{12}In(CO)_{28}]^n$ with Lorenzian interpolation (FWHM = 10 cm^{-1}). Two different views are provided.

IR and ESI mass spectra for $[Rh_6(CO)_{15}InCl_3]^{2-}$ (2).

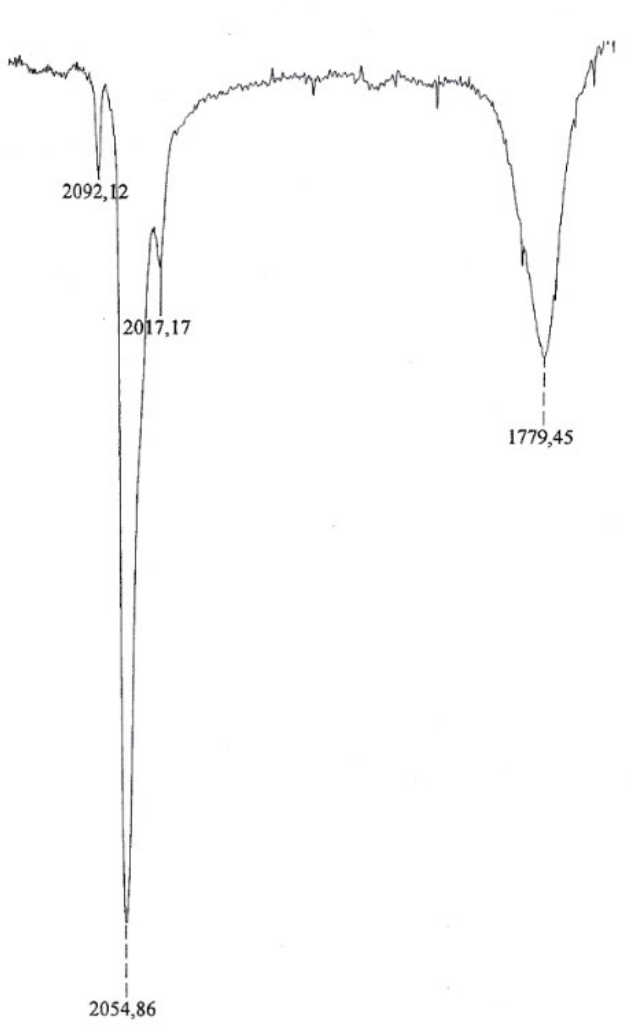

Figure S2a. IR spectrum of $[Rh_6(CO)_{15}InCl_3][NEt_4]_2 \cdot CH_3CN$ registered in EtOH solution.

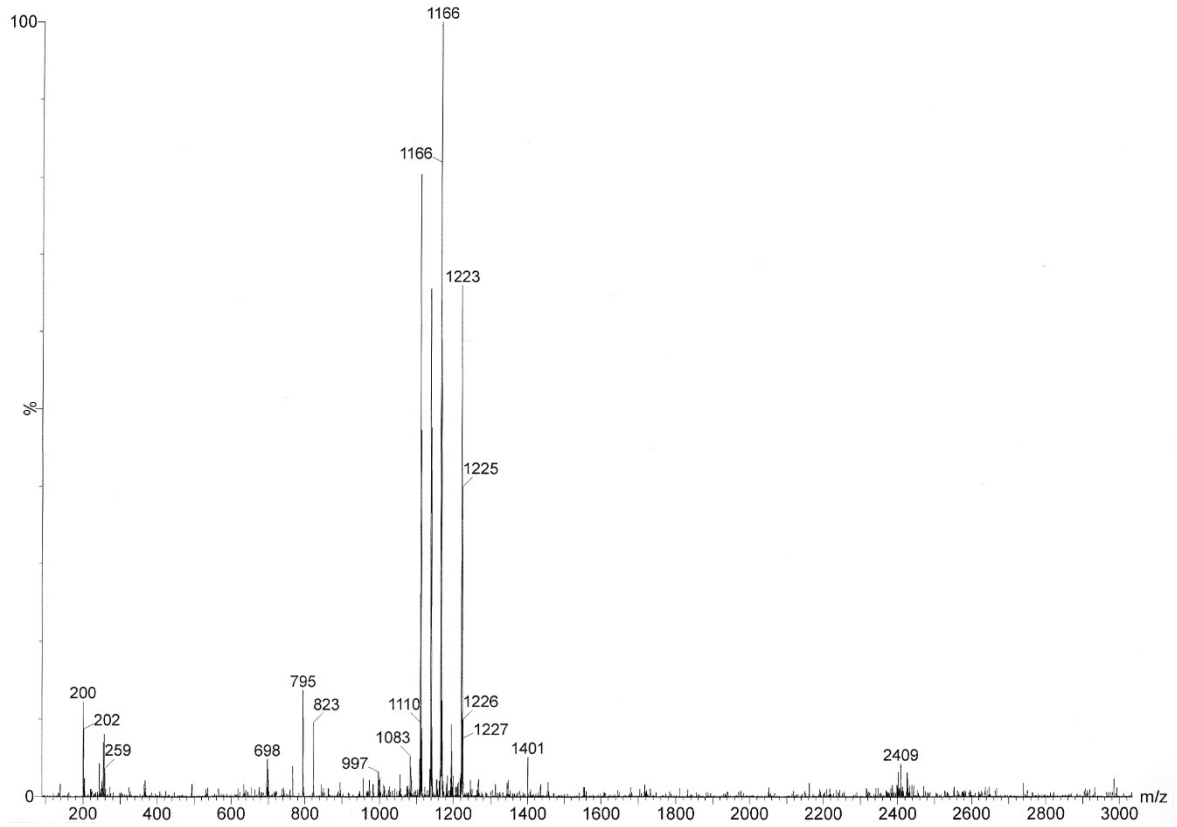

Figure S2b. ESI-MS of $[Rh_6(CO)_{15}InCl_3][NEt_4]_2 \cdot CH_3CN$ registered in CH_3CN solution.

Most relevant signals (m/z)	Corresponding Ions
1223-1194-1166-1138-1110-1083	$[Rh_6(CO)_{15\text{-}14\text{-}13\text{-}12\text{-}11\text{-}10}InCl_2]^-$
823-795	$[Rh_5(CO)_{11\text{-}10}]^-$

Table S2. ESI-MS peak assignments for $[Rh_6(CO)_{15}InCl_3][NEt_4]_2 \cdot CH_3CN$

IR and ESI mass spectra for $[\{Rh_6(CO)_{15}InCl_2\}_2]^{2-}$ (3).

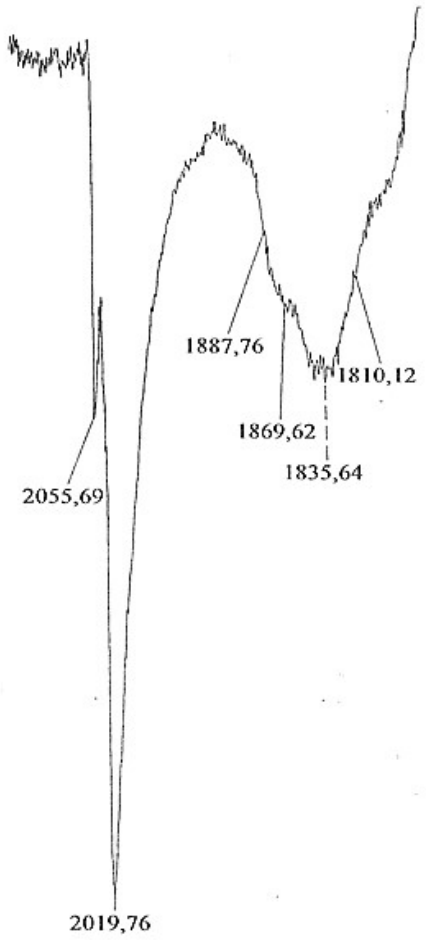

Figure S3a. IR spectrum of $[\{Rh_6(CO)_{15}InCl_2\}_2][NEt_4]_2 \cdot 2THF \cdot 2H_2O$ registered in CH_3CN solution.

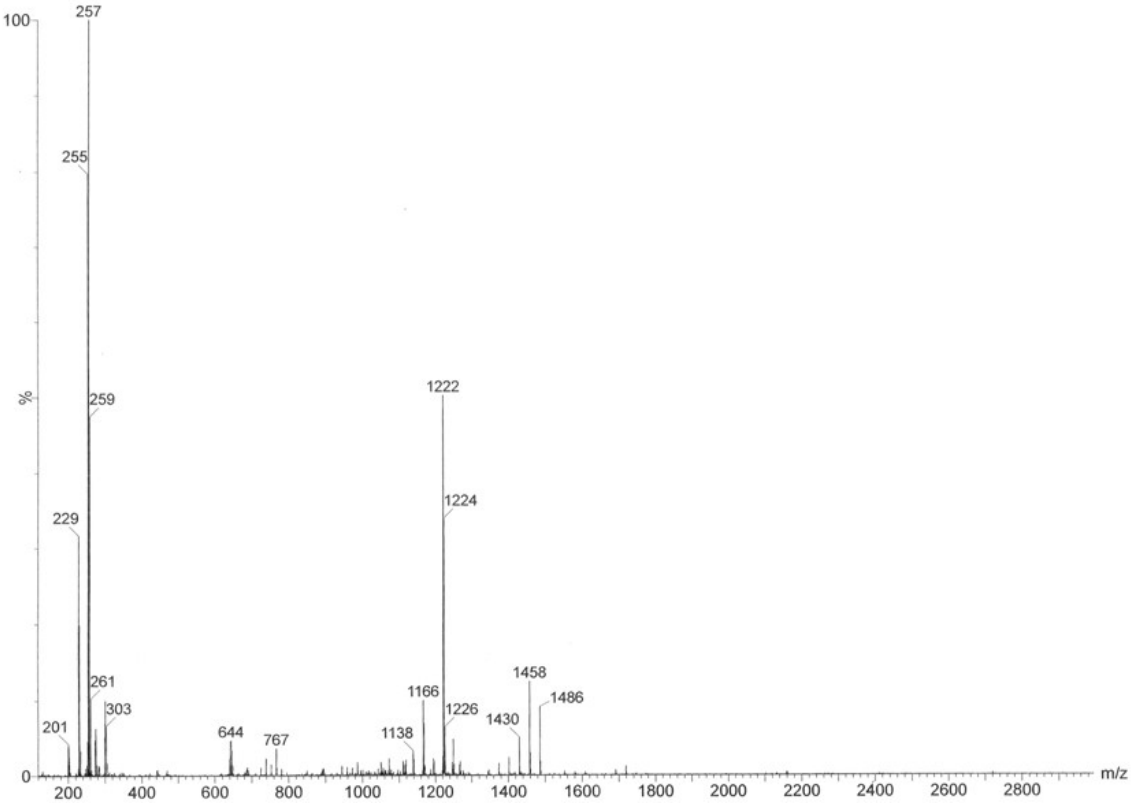

Figure S3b. ESI-MS of $[\{Rh_6(CO)_{15}InCl_2\}_2][NEt_4]_2 \cdot 2THF \cdot 2H_2O$ registered in CH_3CN solution.

Most relevant signals (m/z)	Corresponding Ions
1486-1458-1430-1402-1374	$[Rh_9(CO)_{20\text{-}19\text{-}18\text{-}17\text{-}16}]^-$
1222-1194-1166-1138-1110	$[Rh_6(CO)_{15\text{-}14\text{-}13\text{-}12\text{-}11}InCl_2]^-$
257	$[InCl_4]^-$

Table S3. ESI-MS peak assignments for $[\{Rh_6(CO)_{15}InCl_2\}_2][NEt_4]_2 \cdot 2THF \cdot 2H_2O$.

Table S4. Crystallographic data for clusters **1**, **2** (crystallized in acetonitrile and acetone), and **3**.

Compound	**1**$[NEt_4]_3$	**2**$[NEt_4]_2 \cdot CH_3CN$	**2**$[NEt_4]_2 \cdot (CH_3)_2CO$	**3**$[NEt_4]_2 \cdot 2THF \cdot 2H_2O$
Formula	$C_{52}H_{60}InN_3O_{28}Rh_{12}$	$C_{33}H_{43}Cl_3InN_3O_{15}Rh_6$	$C_{34}H_{46}Cl_3InN_2O_{16}Rh_6$	$C_{54}H_{60}Cl_4In_2N_2O_{34}Rh_{12}$
Fw	2524.77	1560.33	1577.36	2887.40
Crystal system	Trigonal	Orthorhombic	Orthorhombic	Monoclinic
Space group	*R*-3c	*P*nma	*P*nma	$P2_1/n$
a (Å)	23.1561(19)	19.6586(11)	19.5591(11)	17.3907(18)
b (Å)	23.1561(19)	18.1826(10)	17.8943(10)	10.0530(11)
c (Å)	22.053(3)	13.5943(7)	13.8681(8)	22.894(2)
α (°)	90	90	90	90
β (°)	90	90	90	95.836(3)
γ (°)	120	90	90	90
Cell volume ($Å^3$)	10241(2)	4859.2(5)	4859.2(5)	3981.8(7)
Z	6	4	4	2
D (g/cm^3)	2.456	2.133	2.159	2.408
μ (mm^{-1})	3.229	2.680	2.685	3.197
F(000)	7236	3008	3048	2752
θ limits (deg)	1.372 to 24.980	2.138 to 25.000	1.800 to 24.998	1.549 to 24.999
Index ranges	-27<=h<=27, -27<=k<=27, -26<=l<=26	-23<=h<=23, -21<=k<=21, -16<=l<=16	-23<=h<=23, -21<=k<=21, -16<=l<=16	-20<=h<=20, -11<=k<=11, -27<=l<=27
Reflections collected	40411	55592	56365	46627
Independent reflections	2007 [R(int) = 0.0928]	4395 [R(int) = 0.0188]	4429 [R(int) = 0.0602]	7002 [R(int) = 0.0801]
Completeness to θ max	100.0%	99.3 %	99.9 %	100.0 %
Data/restraints/ parameters	2007 / 166 / 151	4395 / 0 / 300	4429 / 66 / 305	7002 / 199 / 497
Goodness of fit	1.390	1.367	1.204	1.144
R_1 ($I > 2\sigma(I)$)	0.1290	0.0184	0.0450	0.0611
wR_2 (all data)	0.2608	0.0452	0.0838	0.1326
Largest diff. peak and hole, e $Å^{-3}$	2.302 and -2.803	0.471 and -0.812	1.181 and -1.302	1.604 and -1.955

Most relevant bond distances for $[Rh_{12}In(CO)_{28}]^{3-}$ (1).

In(1)-Rh(2)#1	2.7668(18)
In(1)-Rh(2)#2	2.7668(18)
In(1)-Rh(2)#3	2.7668(18)
In(1)-Rh(2)#4	2.7668(18)
In(1)-Rh(2)	2.7668(18)
In(1)-Rh(2)#5	2.7670(18)
In(1)-Rh(1)#5	2.8850(19)
In(1)-Rh(1)#3	2.8850(19)
In(1)-Rh(1)#4	2.8850(19)

In(1)-Rh(1)	2.8850(19)
In(1)-Rh(1)#2	2.8850(19)
In(1)-Rh(1)#1	2.8850(19)
Rh(1)-Rh(1)#4	2.773(4)
Rh(1)-Rh(2)#4	2.897(3)
Rh(1)-Rh(2)	2.911(3)
Rh(1)-Rh(2)#3	3.011(3)
Rh(2)-Rh(2)#1	3.012(3)
Rh(2)-Rh(2)#2	3.012(3)

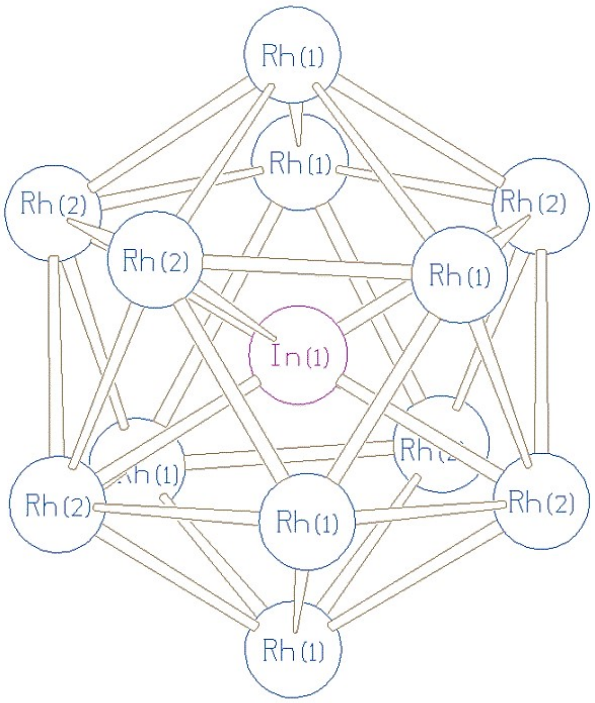

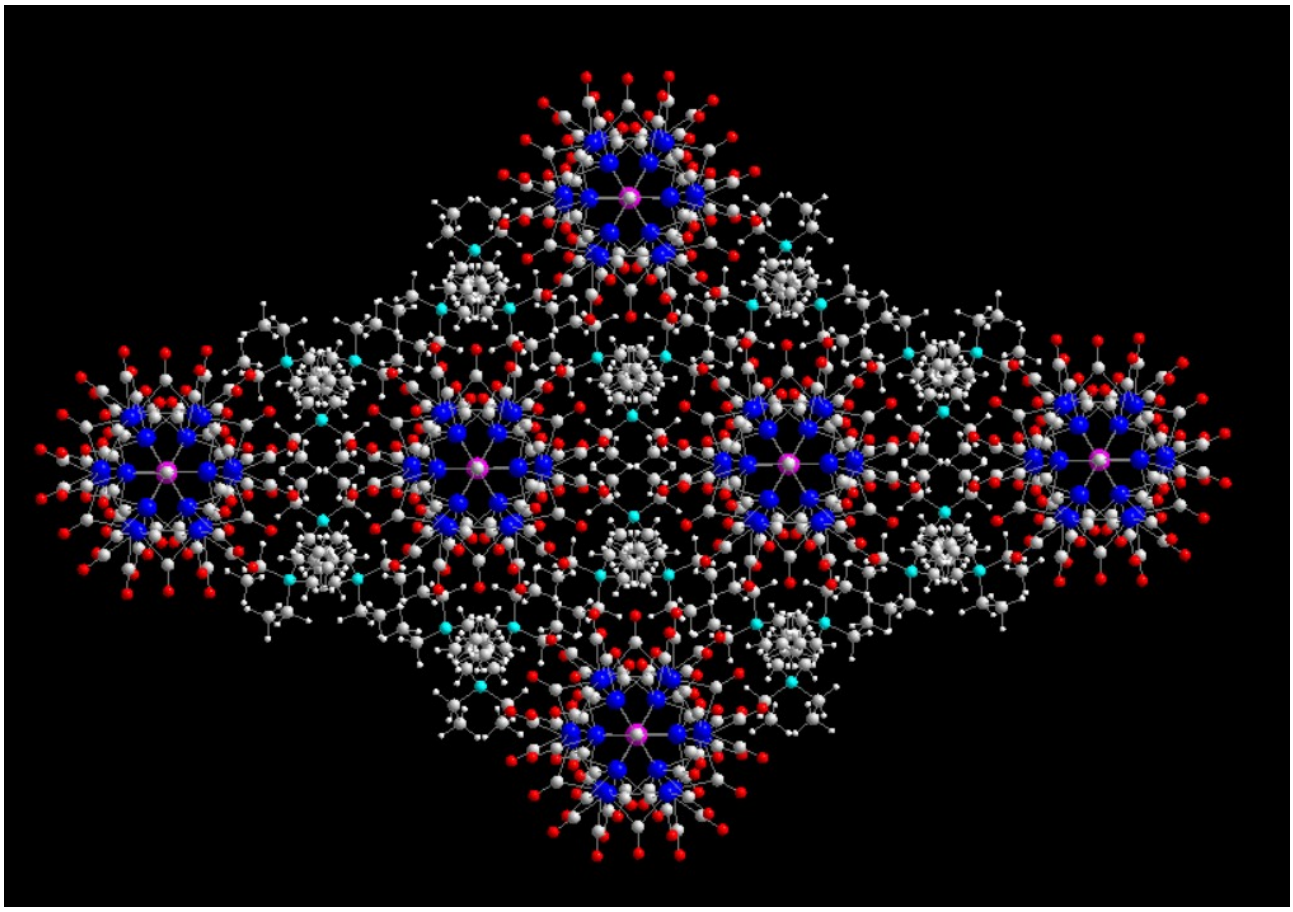

Figure S4a. Solid-state packing of **1** along the *c* axis. Rh atoms in blue, In atoms in magenta, O in red, C in grey, N in cyan, H in white.

Most relevant bond distances for $[Rh_6(CO)_{15}InCl_3]^{2-}$ (2) (crystallized in acetonitrile - A).

Rh(3)-In(5)	2.8366(4)
Rh(4)-In(5)	2.8487(3)
In(5)-Rh(4)#1	2.8488(3)
Rh(1)-Rh(3)	2.7502(3)
Rh(1)-Rh(1)#1	2.7520(4)
Rh(1)-Rh(2)	2.7559(3)
Rh(1)-Rh(4)#1	2.7592(3)
Rh(2)-Rh(1)#1	2.7559(3)
Rh(2)-Rh(4)#1	2.7570(3)

Rh(2)-Rh(4)	2.7571(3)
Rh(3)-Rh(1)#1	2.7501(3)
Rh(3)-Rh(4)#1	2.8330(3)
Rh(3)-Rh(4)	2.8330(3)
Rh(4)-Rh(1)#1	2.7592(3)
Rh(4)-Rh(4)#1	2.8031(4)
In(5)-Cl(2)	2.5001(6)
In(5)-Cl(2)#1	2.5002(6)
In(5)-Cl(1)	2.5183(9)

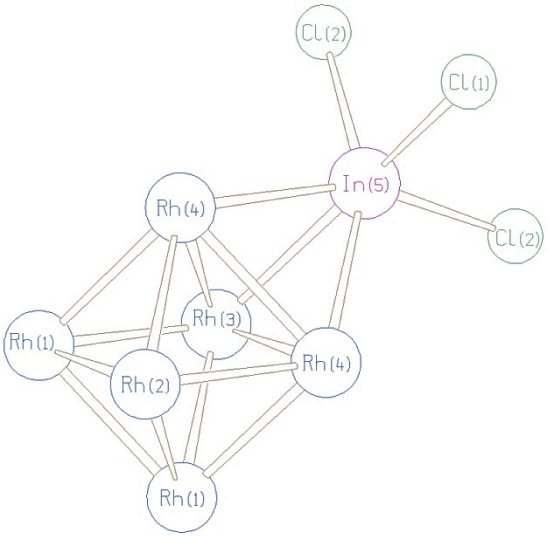

A

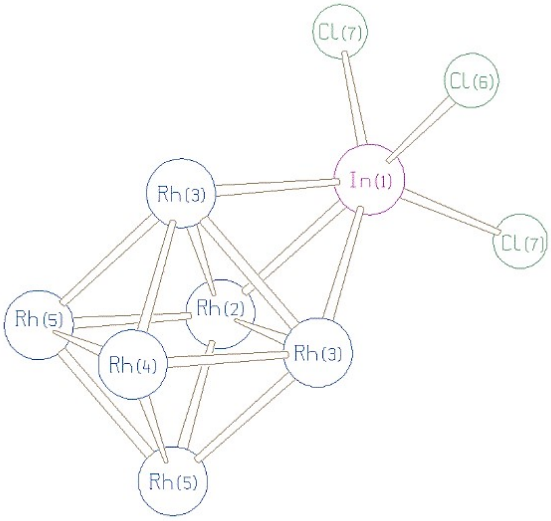

B

Most relevant bond distances for $[Rh_6(CO)_{15}InCl_3]^{2-}$ (2) (crystallized in acetone - B).

In(1)-Rh(2)	2.8275(10)
In(1)-Rh(3)	2.8510(8)
In(1)-Rh(3)#1	2.8511(8)
Rh(2)-Rh(5)#1	2.7381(8)
Rh(2)-Rh(5)	2.7381(8)
Rh(2)-Rh(3)	2.8250(8)
Rh(2)-Rh(3)#1	2.8250(8)
Rh(3)-Rh(4)	2.7545(8)
Rh(3)-Rh(5)#1	2.7615(7)

Rh(3)-Rh(3)#1	2.7992(10)
Rh(4)-Rh(5)	2.7517(8)
Rh(4)-Rh(5)#1	2.7517(8)
Rh(4)-Rh(3)#1	2.7545(8)
Rh(5)-Rh(5)#1	2.7466(10)
Rh(5)-Rh(3)#1	2.7615(7)
In(1)-Cl(7)	2.4991(16)
In(1)-Cl(7)#1	2.4991(16)
In(1)-Cl(6)	2.509(2)

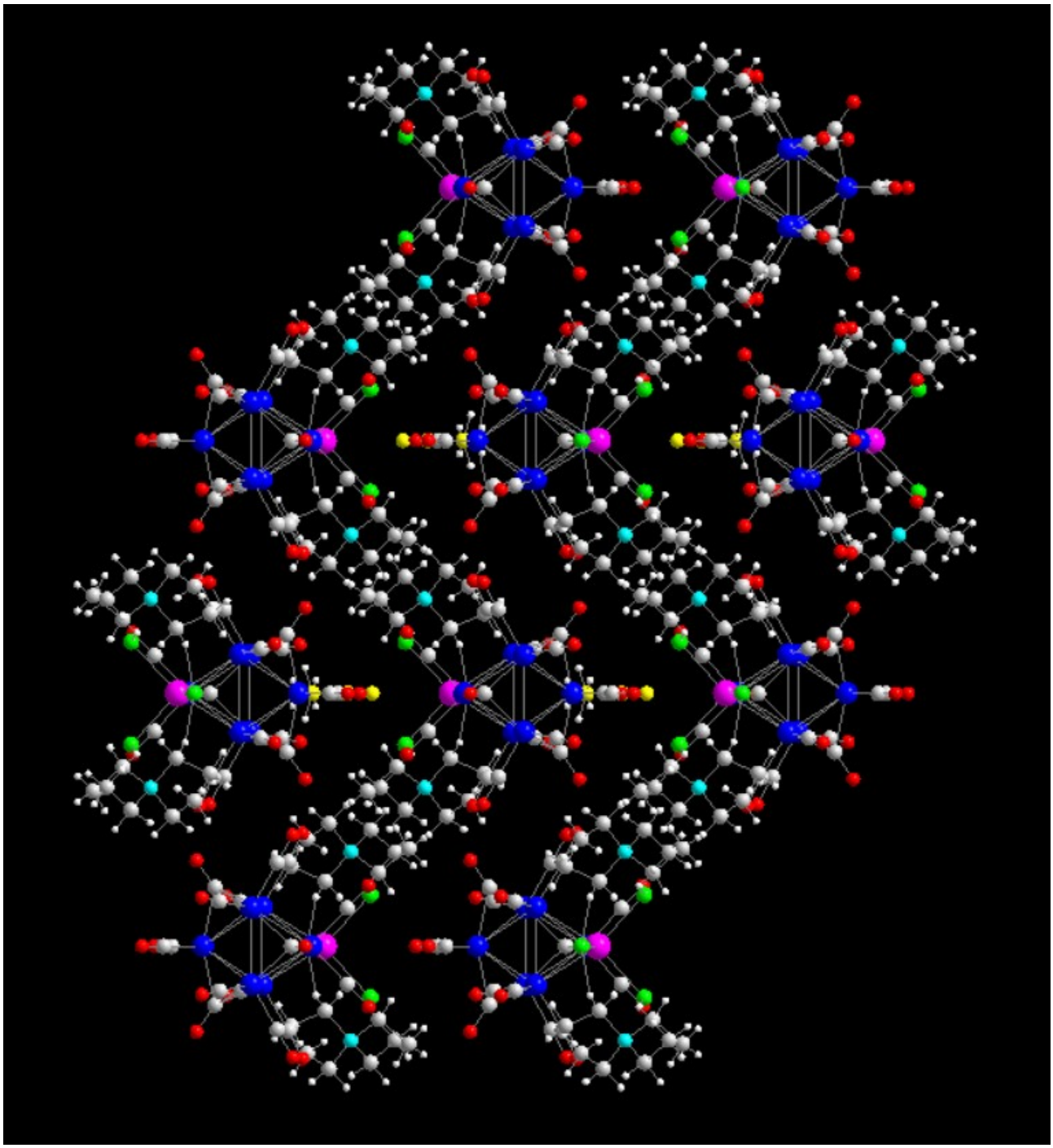

Figure S4b. Solid-state packing of **2** along the *c* axis (crystallized in acetonitrile). Rh atoms in blue, In atoms in magenta, O in red, C in grey, Cl in green, N in cyan, H in white. Yellow atoms belong to the solvent molecules.

Most relevant bond distances for $[\{Rh_6(CO)_{15}InCl_2\}_2]^{2-}$ (3).

In(1)-Rh(2)	2.7610(11)
In(1)-Rh(4)	2.7868(11)
In(1)-Rh(3)	2.8210(12)
Rh(2)-Rh(5)	2.7421(12)
Rh(2)-Rh(6)	2.7513(12)
Rh(2)-Rh(3)	2.8254(12)
Rh(2)-Rh(4)	2.8405(12)
Rh(3)-Rh(7)	2.7601(12)
Rh(3)-Rh(5)	2.7618(12)

Rh(3)-Rh(4)	2.7988(12)
Rh(4)-Rh(6)	2.7437(12)
Rh(4)-Rh(7)	2.7492(12)
Rh(5)-Rh(7)	2.7589(12)
Rh(5)-Rh(6)	2.7618(12)
Rh(6)-Rh(7)	2.7520(12)
In(1)-Cl(9)	2.507(3)
In(1)-Cl(8)	2.601(3)
In(1)-Cl(8)#1	2.673(3)

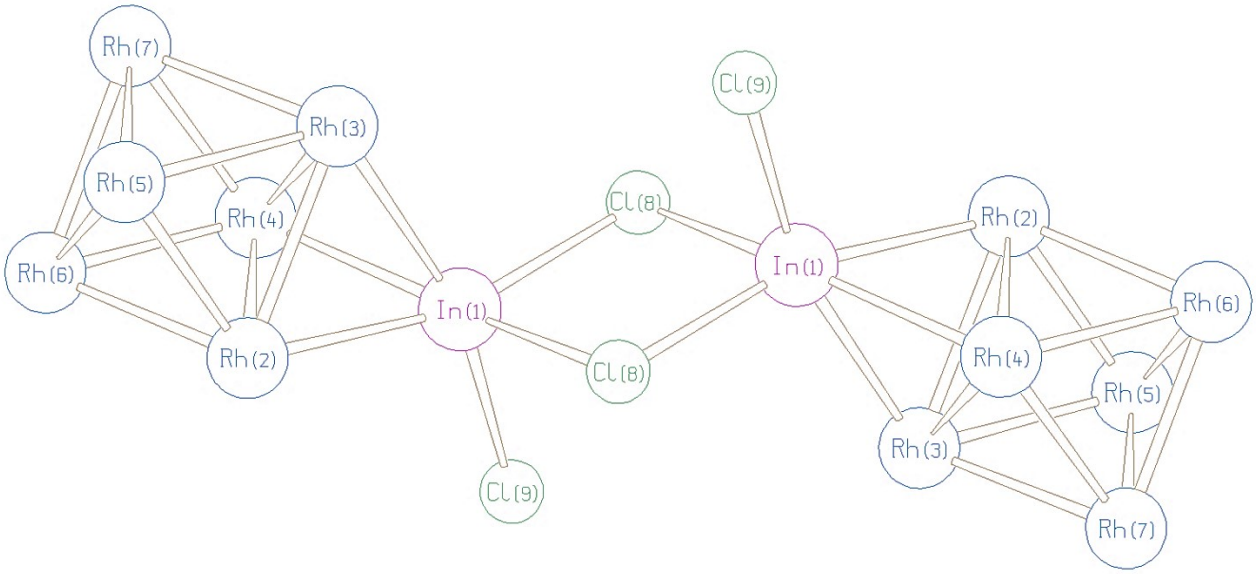

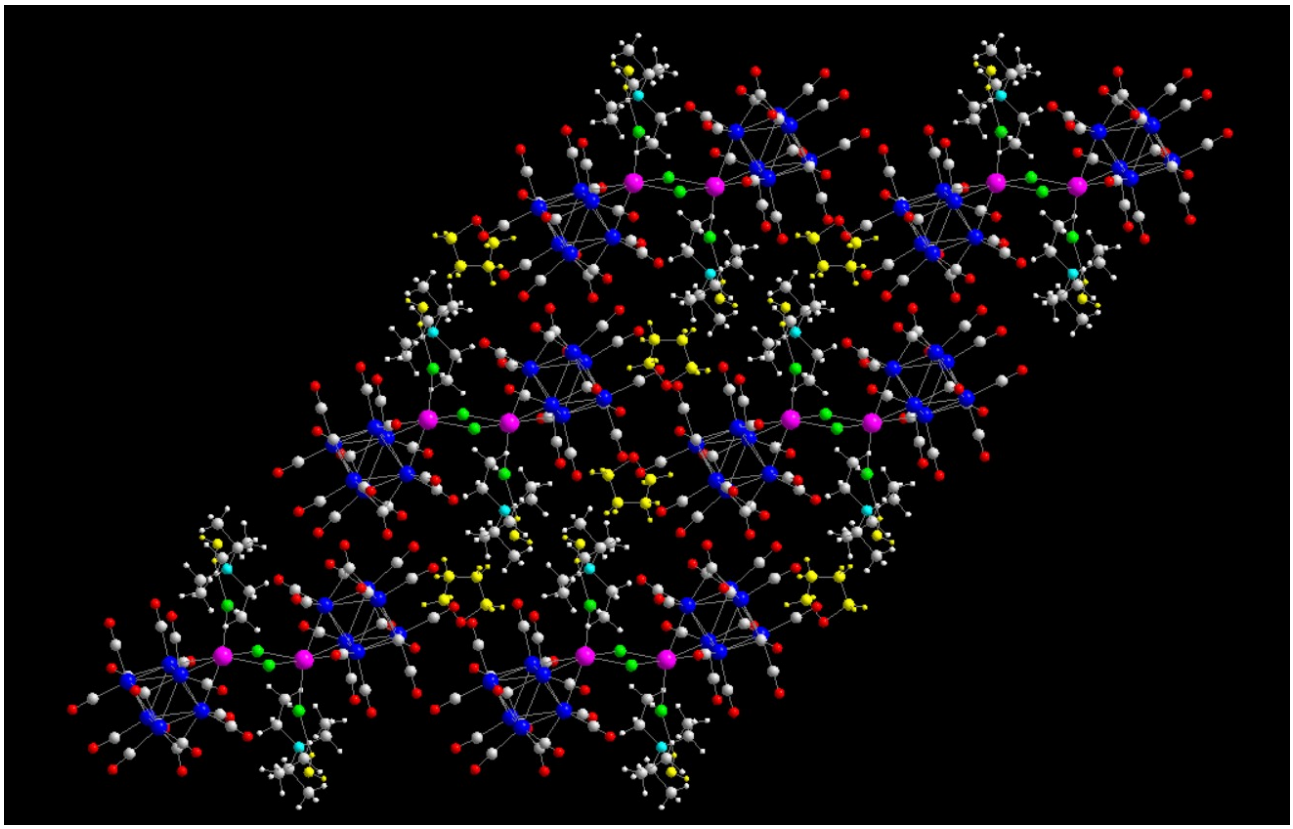

Figure S4c. Solid-state packing of **3** along the *b* axis. Rh atoms in blue, In atoms in magenta, O in red, C in grey, Cl in green, N in cyan, H in white. Yellow atoms belong to the solvent molecules.